An opening crack model for thermo-magneto-electro-elastic solids

Xian-Ci Zhong[1,2,*]

[1] Department of Mathematics and Information Science, Guangxi University,
Nanning Guangxi, 530004, China
[2] Key Laboratory of Disaster Prevention and Structural Safety, Guangxi University,
Nanning Guangxi, 530004, China
* xczhong@gxu.edu.cn, zhongxianci@163.com

Abstract   In previous studies of fracture analysis for a thermo-magneto-electro-elastic solid, the crack-face thermal boundary condition is always assumed to be fully insulated or conductive. In the present paper, an opening crack model is proposed by considering the various physical properties of crack interior. The thermal flux, electric displacement and magnetic induction at the crack surfaces are assumed to be dependent on the crack opening displacement. The effects of applied magneto-electro-mechanical loadings and the thermal conductivity inside a crack on the thermal stress intensity factor are investigated. The obtained results reveal that the thermal stress intensity factor depends not only on applied thermal loadings but also on applied magneto-electro-mechanical loadings and various physical properties of crack interior.

Keywords   Thermo-magneto-electro-elastic solid, Opening crack model, Thermal stress intensity factor

1. Introduction

Due to the giant magnetoelectric coupling effects, magnetoelectroelastic materials own significant technological promise in manufacturing the novel multifunctional devices [1]. Moreover, since the temperature change will affect the overall performance of the smart devices, it is important to investigate the responses of magnetoelectroelastic materials under a thermal loading [2-4]. It is noted that the fracture analysis of a cracked thermo-magneto-electro-elastic solid has attracted much attention [5-9]. One can see that the thermal boundary condition on the crack surfaces is always assumed to be thermally insulated, and the effects of the thermal properties inside the crack on the crack-tip fields are not considered. Recently, in order to investigate the effects of the medium inside a crack on the thermal stress intensity factor, the thermal-medium crack model has been proposed [10]. The obtained results have also revealed that applied mechanical loadings have great influences on the thermal stress intensity factor. On the other hand, some known observations show that the electric permittivity and magnetic permeability of crack interior cannot be disregarded for the fracture analysis of a cracked magnetoelectroelastic solid [11]. It is also seen that the semi-permeable crack-face magnetoelectric boundary conditions have been proposed [12]. Consequently, to address the effects of various physical properties of medium inside a crack, we propose the following crack-face boundary conditions for a cracked thermo-magneto-electro-elastic solid:

$$D^c = -\varepsilon^c \frac{\Delta\phi}{\Delta u_z}, \quad B^c = -\mu^c \frac{\Delta\varphi}{\Delta u_z}, \quad q^c = -\lambda^c \frac{\Delta\theta}{\Delta u_z} \tag{1}$$

where the constants ε^c, μ^c and λ^c denote the dielectric permittivity, magnetic permeability and thermal conductivity of crack interior and they are given as $\varepsilon^c = \varepsilon_r \varepsilon_0 (\varepsilon_0 = 8.85 \times 10^{-12} F/m)$, $\mu^c = \mu_r \mu_0 (\mu_0 = 1.26 \times 10^{-6} Ns^2/C^2)$ and $\lambda^c = \lambda_r \lambda_0 (\lambda_0 = 0.024 W/Km)$ respectively. D^c, B^c and q^c are the electric displacement, magnetic induction and heat flux at the crack faces respectively. $\Delta\phi, \Delta\varphi$ and $\Delta\theta$ are the jumps of electric potential, magnetic potential and temperature change across the crack, respectively. One can find that eight ideal crack models associated with a

combination of permeable and impermeable thermal-magnetic-electric boundary conditions can be obtained by considering the limiting cases of Eq. (1).

The objective of the present paper is to investigate the dependence of the thermal stress intensity factor on applied magneto-electro-mechanical loadings and various physical properties of crack interior. Applying the boundary conditions in Eq. (1), the stationary behavior of a cracked thermo-magneto-electro-elastic solid is considered under a combination of applied magneto-electro-mechanical loadings and a uniform heat flux. The closed-form solution of the thermal stress intensity factor is obtained. Numerical results are carried out to show the variations of the thermal stress intensity factor on applied magneto-electro-mechanical loadings and various physical properties of crack interior.

2. Basic equations and boundary conditions

Consider that a Griffith crack is embedded in a transversely isotropic magnetoelectroelastic solid with the thermal effect. As shown in Fig. 1, we use Cartesian coordinates system xoz and assume that the crack is located at $-a < x < a$. Applied thermo-magneto-electro-mechanical loadings σ_0, D_0, B_0, q_0 are acting on the crack surfaces. Using the boundary conditions in Eq. (1), we have

$$\sigma_{zz}(x,0) = -\sigma_0, \qquad D_z(x,0) = -(D_0 - D^c), \qquad -a < x < a \qquad (2)$$

$$B_z(x,0) = -(B_0 - B^c), \qquad q_z(x,0) = -(q_0 - q^c), \qquad -a < x < a \qquad (3)$$

Hereafter $\sigma_{ij}, D_i, B_i, q_i$ stand for the components of stress, electric displacement, magnetic induction and heat flux.
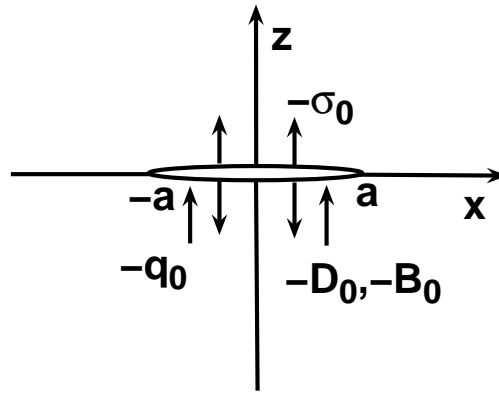
Figure 1. An opening crack in a thermo-magneto-electro-elastic solid

Under the assumption of plane deformation and linear thermo-magneto-electro-elasticity, the constitute equations can be written as

$$\sigma_{xx} = c_{11} \frac{\partial u_x}{\partial x} + c_{13} \frac{\partial u_z}{\partial z} + e_{31} \frac{\partial \phi}{\partial z} + h_{31} \frac{\partial \varphi}{\partial z} - \beta_x \theta \qquad (4)$$

$$\sigma_{zz} = c_{13} \frac{\partial u_x}{\partial x} + c_{33} \frac{\partial u_z}{\partial z} + e_{33} \frac{\partial \phi}{\partial z} + h_{33} \frac{\partial \varphi}{\partial z} - \beta_z \theta \qquad (5)$$

$$\sigma_{xz} = c_{44} \left(\frac{\partial u_x}{\partial z} + \frac{\partial u_z}{\partial x} \right) + e_{15} \frac{\partial \phi}{\partial x} + h_{15} \frac{\partial \varphi}{\partial x} \qquad (6)$$

$$D_x = e_{15} \left(\frac{\partial u_x}{\partial z} + \frac{\partial u_z}{\partial x} \right) - \varepsilon_{11} \frac{\partial \phi}{\partial x} - d_{11} \frac{\partial \varphi}{\partial x} \qquad (7)$$

$$D_z = e_{31} \frac{\partial u_x}{\partial x} + e_{33} \frac{\partial u_z}{\partial z} - \varepsilon_{33} \frac{\partial \phi}{\partial z} - d_{33} \frac{\partial \varphi}{\partial z} + p_z \theta \tag{8}$$

$$B_x = h_{15} \left(\frac{\partial u_x}{\partial z} + \frac{\partial u_z}{\partial x} \right) - d_{11} \frac{\partial \phi}{\partial x} - \mu_{11} \frac{\partial \varphi}{\partial x} \tag{9}$$

$$B_z = h_{31} \frac{\partial u_x}{\partial x} + h_{33} \frac{\partial u_z}{\partial z} - d_{33} \frac{\partial \phi}{\partial z} - \mu_{33} \frac{\partial \varphi}{\partial z} + m_z \theta \tag{10}$$

where u_i, ϕ, φ and θ are the components of elastic displacement, electric potential, magnetic potential and temperature change. $c_{ij}, e_{ij}, h_{ij}, \varepsilon_{ij}, d_{ij}, \mu_{ij}, p_z$ and m_z are the elastic, piezoelectric, piezomagnetic, dielectric permittivity, magnetoelectric, magnetic permeability, pyroelectric and pryomagnetic constants, respectively. β_x and β_z are the stress-temperature coefficient. Application of the equilibrium equation leads to the following partial differential equations

$$c_{11} u_{x,xx} + c_{44} u_{x,zz} + (c_{13} + c_{44}) u_{z,xz} + (e_{31} + e_{15}) \phi_{,xz} + (h_{31} + h_{15}) \varphi_{,xz} = \beta_x \theta_{,x} \tag{11}$$

$$c_{44} u_{z,xx} + c_{33} u_{z,zz} + (c_{13} + c_{44}) u_{x,xz} + e_{15} \phi_{,xx} + e_{33} \phi_{,zz} + h_{15} \varphi_{,xx} + h_{33} \varphi_{,zz} = \beta_x \theta_{,z} \tag{12}$$

$$e_{15} u_{z,xx} + e_{33} u_{z,zz} + (e_{31} + e_{15}) u_{x,xz} - \varepsilon_{11} \phi_{,xx} - \varepsilon_{33} \phi_{,zz} - d_{11} \varphi_{,xx} - d_{33} \varphi_{,zz} = -p_z \theta_{,z} \tag{13}$$

$$h_{15} u_{z,xx} + h_{33} u_{z,zz} + (h_{31} + h_{15}) u_{x,xz} - d_{11} \phi_{,xx} - d_{33} \phi_{,zz} - \mu_{11} \varphi_{,xx} - \mu_{33} \varphi_{,zz} = -m_z \theta_{,z} \tag{14}$$

On the other hand, from the theory of the Fourier heat conduction, one has the following constitute and equilibrium equations

$$q_x = -\lambda_x \frac{\partial \theta}{\partial x}, \qquad q_z = -\lambda_z \frac{\partial \theta}{\partial z}, \qquad \frac{\partial q_x}{\partial x} + \frac{\partial q_z}{\partial z} = 0 \tag{15}$$

Then it follows that

$$\lambda^2 \frac{\partial^2 \theta}{\partial x^2} + \frac{\partial^2 \theta}{\partial z^2} = 0, \qquad \lambda = \sqrt{\frac{\lambda_x}{\lambda_z}}. \tag{16}$$

3. Thermal stress intensity factor

Since the considered problem is linear and only related to the stationary behavior of a cracked thermo-magneto-electro-elastic solid, the magnetoelectroelastic field can be obtained by considering the superposition of that induced by applied magneto-electro-mechanical loadings and that induced by applied uniform heat flux. For the temperature field, similar to those given in [13], one can easily obtain the jump of temperature change across the crack as

$$\theta(x,0) = -\frac{q_0 - q^c}{\lambda \lambda_z} \sqrt{a^2 - x^2}, \qquad -a < x < a. \tag{17}$$

Moreover, using the known results in [12], we give the jump of elastic displacement across the crack, namely

$$u_z(x,0) = \frac{\sigma_0}{\sum_{j=1}^{4} \beta_{1j} a_j} \sum_{j=1}^{4} \eta_{3j} \alpha_j a_j \sqrt{a^2 - x^2}, \qquad -a < x < a \tag{18}$$

where the constants $\beta_{kj}, \alpha_j, a_j$ and η_{3j} are defined as those given in [12]. From the third relation in Eq. (1), Eqs. (17) and (18), the heat flux q^c can be calculated as

$$q^c = \frac{\lambda^c q_0 \sum_{j=1}^{4} \beta_{1j} a_j}{\lambda^c \sum_{j=1}^{4} \beta_{1j} a_j + \lambda \lambda_z \sigma_0 \sum_{j=1}^{4} \eta_{3j} \alpha_j a_j} \qquad \text{for } \sigma_0 \neq 0, \tag{19}$$

$$q^c = \frac{\lambda^c q_0 \sum_{j=1}^{4} \beta_{4j} a_j}{\lambda^c \sum_{j=1}^{4} \beta_{4j} a_j + \lambda \lambda_z (D_0 - D^c) \sum_{j=1}^{4} \eta_{3j} \alpha_j a_j} \quad \text{for} \quad \sigma_0 = 0, D_0 \neq 0, \quad (20)$$

$$q^c = \frac{\lambda^c q_0 \sum_{j=1}^{4} \beta_{6j} a_j}{\lambda^c \sum_{j=1}^{4} \beta_{6j} a_j + \lambda \lambda_z (B_0 - B^c) \sum_{j=1}^{4} \eta_{3j} \alpha_j a_j} \quad \text{for} \quad \sigma_0 = 0, B_0 \neq 0. \quad (21)$$

As observed in [10], the heat flux q^c is dependent on the material properties, applied mechanical loading and thermal conductivity of crack interior. In addition, applied magnetoelectric loadings, electric permittivity and magnetic permeability of crack interior also have influences on the heat flux q^c since they may affect crack opening displacement. Moreover, when $\lambda^c = 0$, one has $q^c = 0$ and the crack is thermally insulated. When $\lambda^c \to \infty$, we get $q^c = q_0$ and the crack is fully conductive.

On the other hand, we can give the explicit solution of the stress field near the crack tip induced by applied uniform heat flux. For saving spaces, we neglect the detail solution procedure and give the thermal stress intensity factor as

$$K_{II} = -\frac{\kappa(q_0 - q^c)a}{2\lambda\lambda_z} \sqrt{\pi a} \sum_{j=1}^{4} \beta_{2j} b_{j1}, \quad (22)$$

where

$$[b_{kj}]_{4\times4} = \begin{bmatrix} 1 & 1 & 1 & 1 \\ \beta_{11} & \beta_{12} & \beta_{13} & \beta_{14} \\ \beta_{41} & \beta_{42} & \beta_{43} & \beta_{44} \\ \beta_{61} & \beta_{62} & \beta_{63} & \beta_{64} \end{bmatrix}^{-1}. \quad (23)$$

The constant κ is only related to the material properties and it can be calculated as

$$\kappa = \frac{M_1 \sum_{j=1}^{4} \beta_{2j} b_{j1} - \kappa_1 \sum_{j=1}^{4} \beta_{2j} b_{j2} - \kappa_2 \sum_{j=1}^{4} \beta_{2j} b_{j3} - \kappa_3 \sum_{j=1}^{4} \beta_{2j} b_{j4}}{\sum_{j=1}^{4} \beta_{2j} b_{j1}}, \quad (24)$$

with

$$\begin{bmatrix} M_1 \\ M_2 \\ M_3 \\ M_4 \end{bmatrix} = \begin{bmatrix} c_{11} - \lambda^2 c_{44} & -(c_{13} + c_{44})\lambda & -(e_{31} + e_{15})\lambda & -(h_{31} + h_{15})\lambda \\ (c_{13} + c_{44})\lambda & c_{44} - c_{33}\lambda^2 & e_{15} - e_{33}\lambda^2 & h_{15} - h_{33}\lambda^2 \\ -(e_{31} + e_{15})\lambda & e_{33}\lambda^2 - e_{15} & \varepsilon_{11} - \varepsilon_{33}\lambda^2 & d_{11} - d_{33}\lambda^2 \\ -(h_{31} + h_{15})\lambda & h_{33}\lambda^2 - h_{15} & d_{11} - d_{33}\lambda^2 & \mu_{11} - \mu_{33}\lambda^2 \end{bmatrix} \begin{bmatrix} \beta_x \\ \beta_z \lambda \\ p_z \lambda \\ m_z \lambda \end{bmatrix}, \quad (25)$$

$$\kappa_1 = c_{13} M_1 - c_{33} M_2 \lambda - e_{33} M_3 \lambda - h_{33} M_4 \lambda - \beta_z, \quad (26)$$

$$\kappa_2 = e_{31} M_1 - e_{33} M_2 \lambda + \varepsilon_{33} M_3 \lambda + d_{33} M_4 \lambda + p_z, \quad (27)$$

$$\kappa_3 = h_{31} M_1 - h_{33} M_2 \lambda + d_{33} M_3 \lambda + \mu_{33} M_4 \lambda + m_z. \quad (28)$$

It is seen that the thermal stress intensity factor K_{II} is dependent on the heat flux at the crack faces q^c. When $q^c = 0$, corresponding to a thermally insulated crack, the thermal stress intensity factor is only dependent on applied thermal loading, material properties and the crack length. When $q^c = q_0$, corresponding to a fully conductive crack, the thermal stress intensity factor is zero. When a crack is full of a medium, the thermal stress intensity factor is dependent on applied thermo-magneto-electro-mechanical loadings and various physical properties of the medium inside the crack. For convenience, the thermal stress intensity factor for $q^c = 0$ is rewritten as K_m and

one get

$$\frac{K_{II}}{K_m} = 1 - \frac{q_c}{q_0}. \tag{29}$$

That is, application of (19)-(21) yields

$$\frac{K_{II}}{K_m} = \frac{\lambda \lambda_z \sigma_0 \sum_{j=1}^{4} \eta_{3j} \alpha_j a_j}{\lambda^c \sum_{j=1}^{4} \beta_{1j} a_j + \lambda \lambda_z \sigma_0 \sum_{j=1}^{4} \eta_{3j} \alpha_j a_j} \quad \text{for} \quad \sigma_0 \neq 0, \tag{30}$$

$$\frac{K_{II}}{K_m} = \frac{\lambda \lambda_z (D_0 - D^c) \sum_{j=1}^{4} \eta_{3j} \alpha_j a_j}{\lambda^c \sum_{j=1}^{4} \beta_{4j} a_j + \lambda \lambda_z (D_0 - D^c) \sum_{j=1}^{4} \eta_{3j} \alpha_j a_j} \quad \text{for} \quad \sigma_0 = 0, D_0 \neq 0, \tag{31}$$

$$\frac{K_{II}}{K_m} = \frac{\lambda \lambda_z (B_0 - B^c) \sum_{j=1}^{4} \eta_{3j} \alpha_j a_j}{\lambda^c \sum_{j=1}^{4} \beta_{6j} a_j + \lambda \lambda_z (B_0 - B^c) \sum_{j=1}^{4} \eta_{3j} \alpha_j a_j} \quad \text{for} \quad \sigma_0 = 0, B_0 \neq 0. \tag{32}$$

4. Numerical results and discussions

In order to investigate the effects of applied magneto-electro-mechanical loadings and the physical properties of crack interior on the thermal stress intensity factor, we choose a special thermo-magneto-electro-elastic solid for numerical computations and the material properties are given in Table 1 [3]. For the sake of simplicity, we further suppose that $\varepsilon_r = \mu_r = \lambda_r = \omega$. When $\omega = 0$, the crack is fully thermo-magneto-electric impermeable. When $\omega \to \infty$, the crack is fully thermo-magneto-electric permeable. When $\omega = 1$, the crack is full of air.

Table 1. The material properties

Elastic constants ($\times 10^{10}$ N/m^2)				Piezoelectric constants (C/m^2)			Dielectric permittivity ($\times 10^{-11}$ C^2/Nm^2)	
c_{11}	c_{13}	c_{33}	c_{44}	e_{31}	e_{33}	e_{15}	ε_{11}	ε_{33}
7.41	3.93	8.36	1.32	-0.16	0.347	-0.138	8.26	9.03

Magnetic permeability ($\times 10^{-6}$ Ns^2/C^2)		Electromagnetic constants ($\times 10^{-11}$ Ns/VC)		Piezomagnetic constants (N/Am)		
μ_{11}	μ_{33}	d_{11}	d_{33}	h_{31}	h_{33}	h_{15}
5	10	-3612.68	-2.4735	580.3	699.7	550

Thermal moduli ($\times 10^5$ N/Km^2)		Pyroelectric constant ($\times 10^{-6}$ C/N)	Pyromagnetic constant ($\times 10^{-6}$ N/AKm)	Heat conduction coefficients (W/Km)	
β_x	β_z	p_z	m_z	λ_x	λ_z
6.21	5.51	-2.94	5.187	9	9

Fig. 2 is depicted to show the variation of the normalized thermal stress intensity factor K_{II}/K_m versus ω under the loadings of $\sigma_0 = 10MPa$, $D_0 = 1 \times 10^{-4} C/m^2$ and $B_0 = 0.01 N/Am$. It is seen from Fig. 2 that with the increasing of ω, the normalized thermal stress intensity factor K_{II}/K_m is decreasing rapidly. The phenomenon is in accordance with that given in [10] for an opening crack in a purely elastic material. For $\omega = 0$, one has $K_{II}/K_m = 1$. For $\omega \to \infty$, $K_{II}/K_m = 0$. For a crack full of a medium, the thermal stress intensity factor is located between

that for a fully permeable crack and that for a fully impermeable one. One can see that the thermal stress intensity factor is always overestimated for a thermally insulated crack.
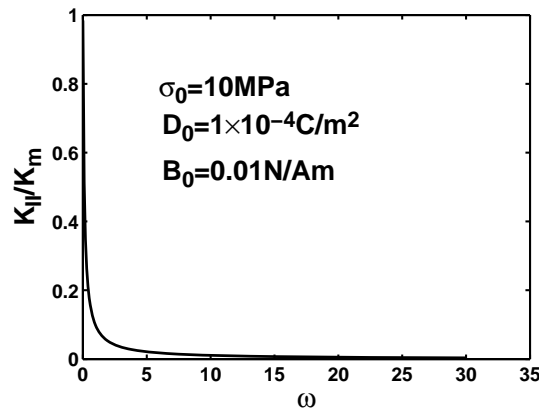
Figure 2. The variations of the normalized thermal stress intensity factor K_{II} / K_m versus ω under the loadings of $\sigma_0 = 10 MPa$, $D_0 = 1 \times 10^{-4} C / m^2$ and $B_0 = 0.01 N / Am$.
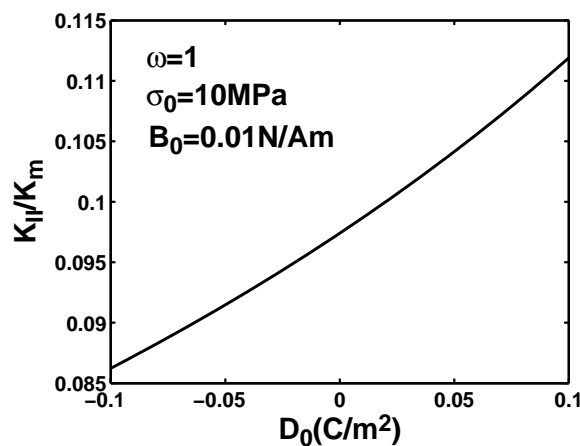
Figure 3. The variations of the normalized thermal stress intensity factor K_{II} / K_m versus D_0 under the loadings of $\sigma_0 = 10 MPa$ and $B_0 = 0.01 N / Am$ for an air crack.

Moreover, for an air crack, it is very interesting to investigate the effects of applied magneto-electro-mechanical loadings on the thermal stress intensity factor, since the important issue is little to be considered in the open literatures [5-9]. Fig. 3 presents the variations of the normalized thermal stress intensity factor K_{II} / K_m versus the electric loading D_0 for $\sigma_0 = 10 MPa$ and $B_0 = 0.01 N / Am$. One can find from Fig. 3 that a positive electric loading enhances the normalized stress intensity factor, and a negative one impedes the normalized stress intensity factor. It is attributed to the fact that for an air crack, a positive electric loading aids the crack opening displacement and a negative one decreases the crack opening displacement [12]. Similarly, it is seen from Fig. 4 that the effects of applied magnetic loadings on the normalized thermal stress intensity factor are in agreement with those of applied electric loadings. On the other hand, Fig. 5 is drawn to show the dependence of the normalized thermal stress intensity factor on applied mechanical loadings. It is found that an increase of applied mechanical loading σ_0 enhances the normalized thermal stress intensity factor, which is similar to the observation in [10]. For a practical situation, always a combination of applied thermo-magneto-electro-mechanical loadings is acting on the smart devices. One can observe from the above phenomena that to address the thermal stresses near the crack tips, the effects of applied magneto-electro-mechanical loadings and the physical properties of crack interior should be considered comprehensively.
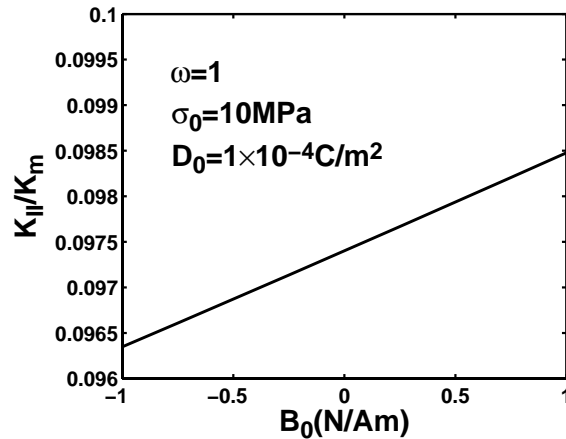
Figure 4. The variations of the normalized thermal stress intensity factor K_{II}/K_m versus B_0 under the loadings of $\sigma_0 = 10MPa$ and $D_0 = 1 \times 10^{-4} C/m^2$ for an air crack.
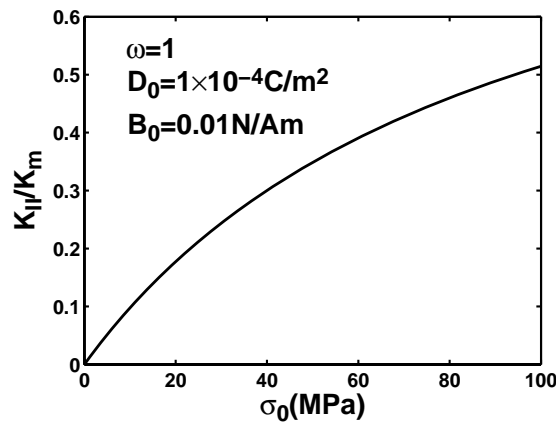
Figure 5. The variations of the normalized thermal stress intensity factor K_{II}/K_m versus σ_0 under the loadings of $D_0 = 1 \times 10^{-4} C/m^2$ and $B_0 = 0.01 N/Am$ for an air crack.

4. Conclusions

To address the effects of various physical properties of crack interior on the thermal stress intensity factor, an opening crack model is proposed in the paper. Eight ideal crack models are the limiting cases of the proposed one. The problem of an opening crack embedded in an infinite thermo-magneto-electro-elastic solid is investigated. The closed-form solution of the thermal stress intensity factor is given. Numerical results are carried to show the influences of applied magneto-electro-mechanical loadings and various physical properties of crack interior on the thermal stress intensity factor. The results reveal that for an opening crack full of a medium, the effects of applied magneto-electro-mechanical loadings and various physical properties of crack interior on the thermal stress intensity factor should be considered. Under the assumption of thermally insulated crack model, the thermal stress intensity factor is always overestimated.

References

[1] C.W. Nan, M.I. Bichurin, S. Dong, D. Viehland, G. Srinivasan, Multiferroic magnetoelectric composites: Historical perspective, status, and future directions. J Appl Phys, 103 (2008) 031101.

[2] M. Aouadi, Some theorems in the generalized theory of thermo-magnetoelectroelasticity under Green–Lindsay's model, Acta Mech, 200 (2008) 25-43.

[3] P. F. Hou , G. H. Teng, H. R. Chen, Three-dimensional Green's function for a point heat source in two-phase transversely isotropic magneto-electro-thermo-elastic material, Mech Mater, 41 (2009) 329-338.

[4] M. I. A. Othman, Generalized electro-magneto thermoelasticity in Case of thermal shock plane waves for a finite conducting half space with two relaxation times. Mech Mech Engng, 14 (2010) 5-30.

[5] C. F. Gao, H. Kessler, H. Balke, Fracture analysis of electromagnetic thermoelastic solids. Eur J Mech A/Solids, 22 (2003) 433-442.

[6] W. Q. Chen, K. Y. Lee, H. J. Ding, General solution for transversely isotropic magneto-electro-thermo-elasticity and the potential theory method. Int J Solids Struct, 42 (2004) 1361-1379.

[7] B. L. Wang, O. P.   Niraula, Transient thermal fracture analysis of transversely isotropic magneto- electro-elastic materials. J Thermal Stresses, 30 (2007) 297–317.

[8] J. Sladek, V. Sladek, P. Solek , Ch. Zhang, Fracture analysis in continuously nonhomogeneous magneto-electro-elastic solids under a thermal load by the MLPG. Int J Solids Struct, 47 (2010) 1381-1391.

[9] W. J. Feng, P. Ma, R.K.L. Su, An electrically impermeable and magnetically permeable interface crack with a contact zone in magnetoelectroelastic bimaterials under a thermal flux and magnetoelectromechanical loads. Int J Solids Struct, 49 (2012) 3472-3483.

[10] X. C. Zhong, K. Y. Lee, A thermal-medium crack model. Mech Mater, 51 (2012) 110-117.

[11] B. L., Wang, Y.W Mai, Applicability of the crack-face electromagnetic boundary conditions for fracture of magnetoelectroelastic materials. Int J Solids Struct 44 (2007) 387–398.

[12] X. C. Zhong, X. F. Li, Magnetoelectroelastic analysis for an opening crack in a piezoelectromagnetic solid, Eur J Mech A/Solids, 26 (2007) 405-417.

[13] Y. M. Tsai, Orthotropic thermoelastic problem of uniform heat flow disturbed by a central crack. J Compos Mater, 18 (1984) 122–131.